JOURNAL OF MATERIALS SCIENCE **39** (2004) 5371 – 5374

Evolution of strain states and textures during roll-cladding in STS/Al/STS sheets

JONG-KOOK KIM, MOO-YOUNG HUH*, JAE-CHUL LEE
Division of Materials Science and Engineering, Korea University, Seoul 136-701, Korea
E-mail: myhuh@korea.ac.kr

KWANG-KOO JEE
Division of Materials, Korea Institute of Science and Technology, Seoul 136-791, Korea

OLAF ENGLER
Hydro Aluminium Deutschland GmbH, R+D Center Bonn, P.O. Box 2468, D–53014 Bonn, Germany

The evolution of strain states and textures during roll-cladding of three plies of sheets comprising ferritic stainless steel (STS), aluminum (Al) and ferritic stainless steel was investigated by measurements of crystallographic textures and by simulations with the finite element method (FEM). Because the deformation mainly occurs in the Al layer during roll-cladding, the present investigation was focused on the Al layer located at the middle of clad samples. Roll-cladding of STS/Al/STS sheets led to the development of a strong through thickness texture gradient in the Al sheet which was characterized by shear textures at the surface layer and rolling textures at the center layer. The temperature of the cladding operation played an important role in the evolution of textures.

1. Introduction

Stainless steel (STS) clad aluminum (Al) sheets comprising STS/Al or STS/Al/STS combine the excellent corrosion-resistant and mechanical properties of stainless steel and the high thermal and electrical conductivities of aluminum. Roll-cladding is the most prevalent process to produce stainless steel clad aluminum sheets because of a fast production rate. During the roll-cladding process, the assembly of STS/Al or STS/Al/STS is heated to the cladding temperature and then inserted jointly into the rolling mill. Since bonding at the interface of STS and Al is obtained during rolling, variations of the stain state in the roll gap are of great importance. Several analytical models for the roll-cladding process have been proposed so far. However, these works focused mainly on the prediction of the rolling pressure and horizontal stress distributions in the overall component layers [1, 2].

In the present work, three plies of sheets comprising two outer surfaces of ferritic stainless steel (STS 430) and inner middle of aluminum alloy (AA 3003) were produced by roll-cladding at 300°C and the evolution of texture and microstructure throughout the sample thickness of AA 3003 was studied in order to examine the variation of strain states during roll-cladding. Furthermore, the strain states during roll cladding were analyzed by the finite element method (FEM), and the strain history data extracted from the FEM computations were also utilized to simulate the deformation textures at various thickness layers.

2. Experimental procedure

In the present study cold rolled STS 430 sheet with a thickness of 0.5 mm and cold rolled and fully recrystallized AA 3003 with a thickness of 3.0 mm were used as initial samples. The assembly of STS 430/AA 3003/STS 430 was prepared and heated to 300°C and then inserted jointly into the rolling mill with a roll diameter of 470 mm. During roll-cladding, the total thickness reduction of the assembly was 30%. While the STS 430 sheets hardly deformed plastically during roll-cladding, the aluminum sheet was thinned to a final gauge of about 2.1 mm.

Pole figure measurements were carried out by means of a conventional X-ray texture goniometer [3]. From three incomplete pole figures, the three-dimensional orientation distribution functions (ODF) $f(g)$ were calculated by the series expansion method according to Bunge ($l_{\max} = 22$) [4]. Most of the pole figures displayed the typical orthotropic symmetry of a rolled sheet; accordingly, the ODFs were calculated in the Euler angle range of $0° \leq \{\varphi_1, \Phi, \varphi_2\} \leq 90°$. To determine the texture variation through the thickness of AA 3003, texture measurements were performed at the surface layer (indicated by the parameter $s = 1.0$)

* Author to whom all correspondence should be addresed.

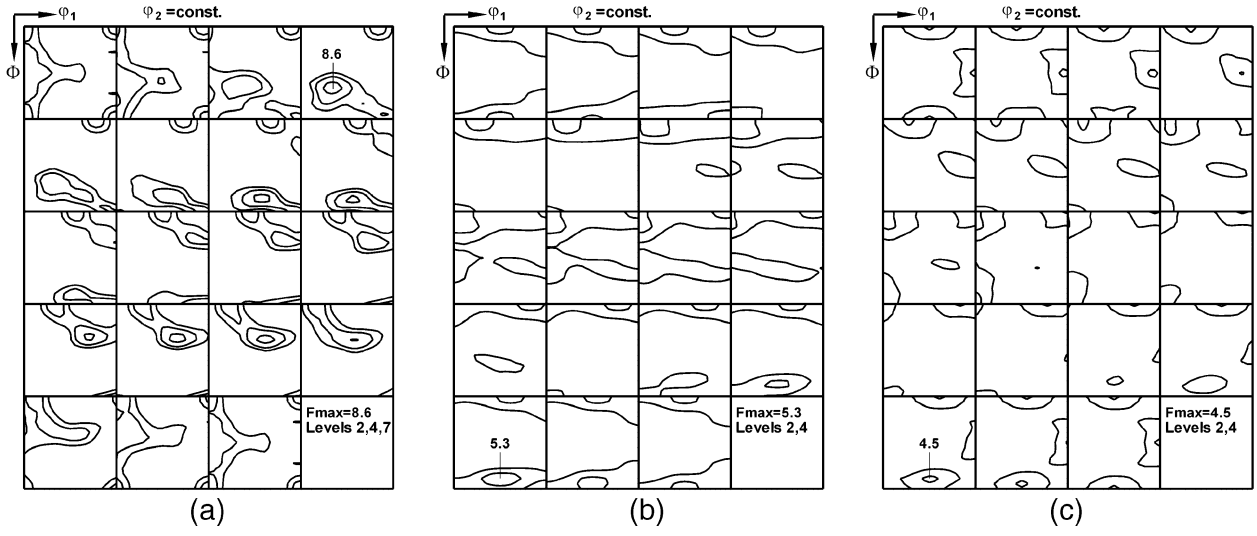

Figure 1 Evolution of through-thickness textures in AA 3003 after roll-cladding: (a) center layer, (b) 2/3 thickness layer, and (c) surface layer.

for the layer in contact with STS 430 and center layer ($s = 0.0$) of the aluminum sheet and 2/3 thickness layer ($s = 0.66$) between the surface and center layer.

3. Results and discussion

As mentioned previously, the clad samples in this work comprised three layers; two outer surfaces of STS 430 and one inner layer of AA 3003. The thermo-mechanical processes involving roll-cladding hardly affected the texture and microstructure of STS 430. In contrast, AA 3003 experienced a remarkable change in the texture and microstructure during roll-cladding. The initial AA 3003 sheets displayed a recrystallized microstructure, consisting of more or less equiaxed grains with a grain size of about 25 μm. All the layers of initial AA 3003 sheet depicted the well-known cube-recrystallization textures which were characterized by preferred cube-orientations with maximum texture intensities of $f(g) \geq 9.0$.

Roll-cladding led to pronounced texture gradients throughout the sample thickness of AA 3003 (Fig. 1). Two types of textures existed in the center layer ($s = 0.0$) of the clad AA 3003 sheets; cube-orientations with intensities of $f(g) \geq 7.0$ and also the preferred orientations assembled along the β-fiber are observed (Fig. 1a). In the 2/3 thickness layer ($s = 0.66$) between the surface and center layer, the typical shear texture of fcc metals was found (Fig. 1b). Here, the maximum texture intensity was obtained in the 45° ND rotated cube orientation $\{001\}\langle 110\rangle$ and pronounced ND-scatters of $\{001\}\langle 100\rangle$ and $\{111\}\langle uvw\rangle$ orientations were also observed. Close to the sheet surfaces ($s = 1.0$) in contact with STS 430, the texture was characterized by the development of two distinct texture components of $\{011\}\langle 011\rangle$ and $\{001\}\langle 110\rangle$ (Fig. 1c).

Similar to the evolution of through thickness texture gradients, AA 3003 at the middle of clad samples displayed different microstructures throughout the thickness after roll-cladding at 300°C. Fig. 2 shows examples of microstructures observed by electron back scattered diffraction (EBSD) in which grain boundaries having misorientation higher than 15° are marked as black lines. As clearly seen in Fig. 2, the microstructure of the surface layer ($s = 1.0$) consisted of small recrystallized grains of about 5.0 μm, while larger grains of about 10 μm were observed in the center layer ($s = 0.0$).

The evolution of strain gradients during roll-cladding was analyzed with the two-dimensional FEM code DEFORM^{TM}-2D[1]. Although the FEM computations are two-dimensional, the geometry convention with X_1 parallel to the rolling direction and X_3 parallel to the sheet normal direction was maintained for convenience. Thus, any deviation from the ideal plane strain condition is manifested in a non-zero strain rate component $\dot{\varepsilon}_{13}$. The variation of the strain state in AA 3003 (material at the middle of clad samples) during the rolling pass for roll-cladding is calculated by FEM and is displayed in Fig. 3 by plotting the strain rates $\dot{\varepsilon}_{11}$ and $\dot{\varepsilon}_{13}$ as a function of the FEM time. Friction coefficients between two interfaces were assumed for the FEM simulations; $\mu_{\text{roll/STS}} = 0.25$ for roll surface and STS 430 and $\mu_{\text{STS/Al}} = 0.25$ for STS 430 and AA 3003. It appears that the shear strain rate $\dot{\varepsilon}_{13}$ in the rolling gap is not homogeneous but varies continuously from the entry to the exit of the roll gap. Note that the first negative maximum of $\dot{\varepsilon}_{13}$ for $s = 1.0$ in Fig. 3b is overstated by contact problems during the FEM simulation, which is not important in the present context. The variation of $\dot{\varepsilon}_{13}$ strongly depends on the through-thickness parameter s in that its maximum amount decreased from the surface to the center layer. Ignoring the first negative maximum of $\dot{\varepsilon}_{13}$, the shear component $\dot{\varepsilon}_{13}$ in the layers $s = 1.0$ and 0.66 shows a strong positive maximum near the entry of the roll gap, turns zero after halfway in between and becomes negative close to the exit of the roll gap. However, the variation of $\dot{\varepsilon}_{13}$ along the stream line of $s = 0.0$ is negligible.

The strain history derived by the FEM simulation was used to model the evolution of deformation texture of AA 3003 accompanying roll-cladding. For that purpose, the initial textures were discretized into sets of

[1] DEFORM is a registered trademark of Scientific Forming Technologies Corporation, Columbus, OH.

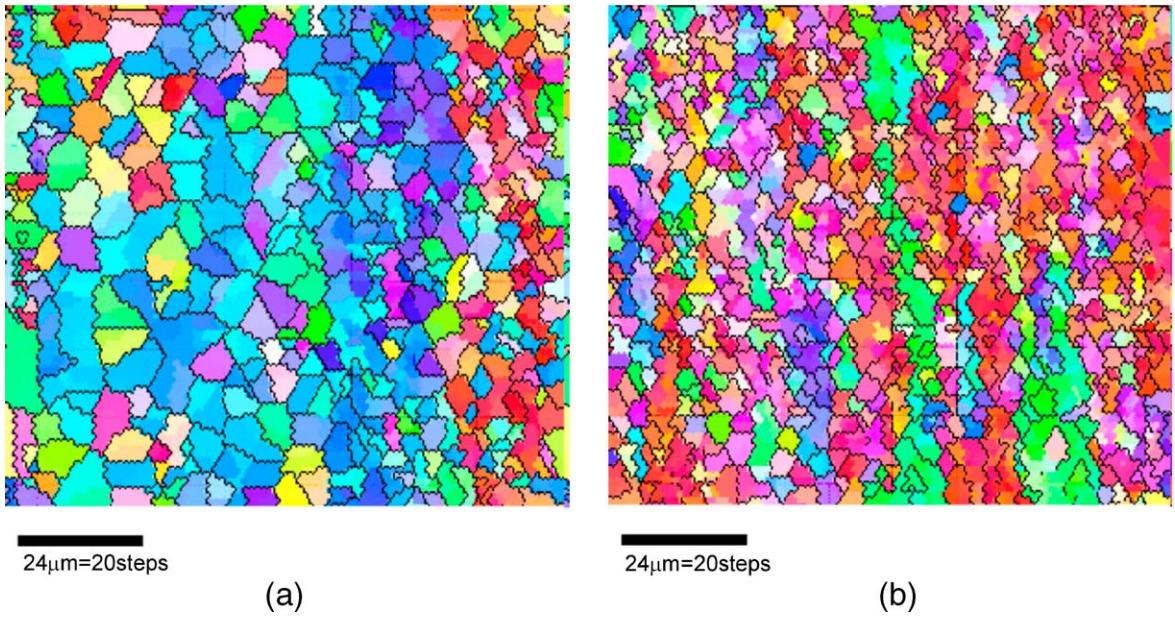

Figure 2 EBSD observed from (a) center layer and (b) surface layer of AA 3003.

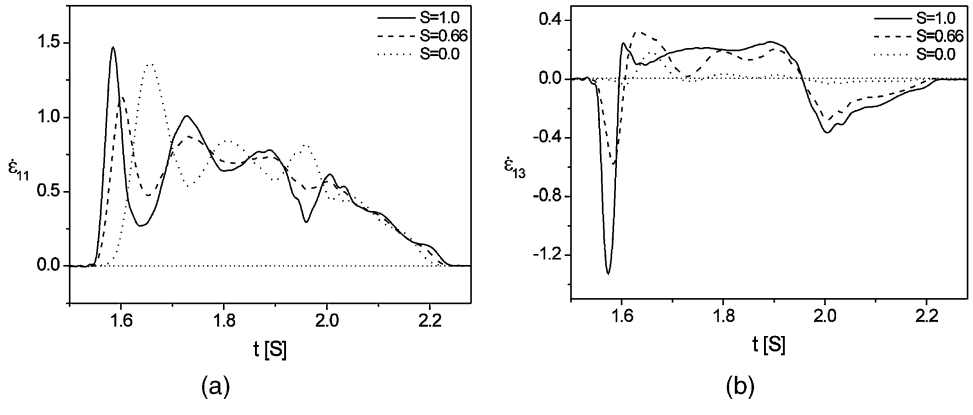

Figure 3 Strain states in a roll gap calculated by FEM simulation: Variation of (a) $\dot{\varepsilon}_{11}$ and (b) $\dot{\varepsilon}_{13}$.

about 4000 individual orientations with equal weights. As described in more detail elsewhere [5], the strain rates $\dot{\varepsilon}_{ij}$ given by the FEM simulations were fed into the full constraint polycrystal deformation model (e.g. [6–8]). The rolling pass for cladding was run in about 30 steps using constant time increments of $\Delta t = 0.023$ s.

The simulated results are shown in Fig. 4 in the form of the ODFs for $s = 0.0$ and $s = 0.66$, respectively. For the sheet center ($s = 0.0$), the typical rolling texture developed, which is typical of an approximate plane strain deformation state. It was noted that textures simulated for $s = 1.0$ and $s = 0.66$ were nearly identical. For both surface layer ($s = 1.0$) and 2/3 thickness layer ($s = 0.66$) pronounced shear textures consisting of {001}⟨110⟩ and {111}⟨uvw⟩ were obtained.

Apparently, some texture components at the various sheet layers obtained experimentally cannot be modeled by the deformation textures for roll-cladding. These discrepancies between the modeled and experimental textures can to a large extent be attributed to the annealing effect during roll-cladding because the samples were heated to 300°C just before rolling. For the sheet center ($s = 0.0$), a mixture of the rolling texture and cube recrystallization texture developed in the experimental texture. The deformation during roll-cladding led to the formation of rolling texture components and subsequently a part of them were recrystallized to develop the cube-texture. For both surface layer ($s = 1.0$) and 2/3 thickness layer ($s = 0.66$) pronounced shear textures consisting of {001}⟨110⟩ and {111}⟨uvw⟩ were obtained. Recently, Engler *et al.* [9] showed that recrystallization nucleation at the grain boundaries gives rise to the occurrence of these texture components in the final recrystallization textures of sheet layers with pronounced shear deformation textures.

Finally, it should be addressed that the formation of strong {011}⟨011⟩ orientation at the surface layer ($s = 1.0$) of AA 3003. This orientation has seldom been reported in rolling and recrystallization textures of aluminium sheets. It is anticipated that orientations with a higher stored energy nucleate more easily than orientations with low stored energy. In the literature on recrystallization textures it is commonly assumed that the stored energy of the various texture components is proportional to their Taylor-factor M (e.g. [9, 10]). In our recent work [9], Taylor-factors M were calculated for the strain conditions for developing the

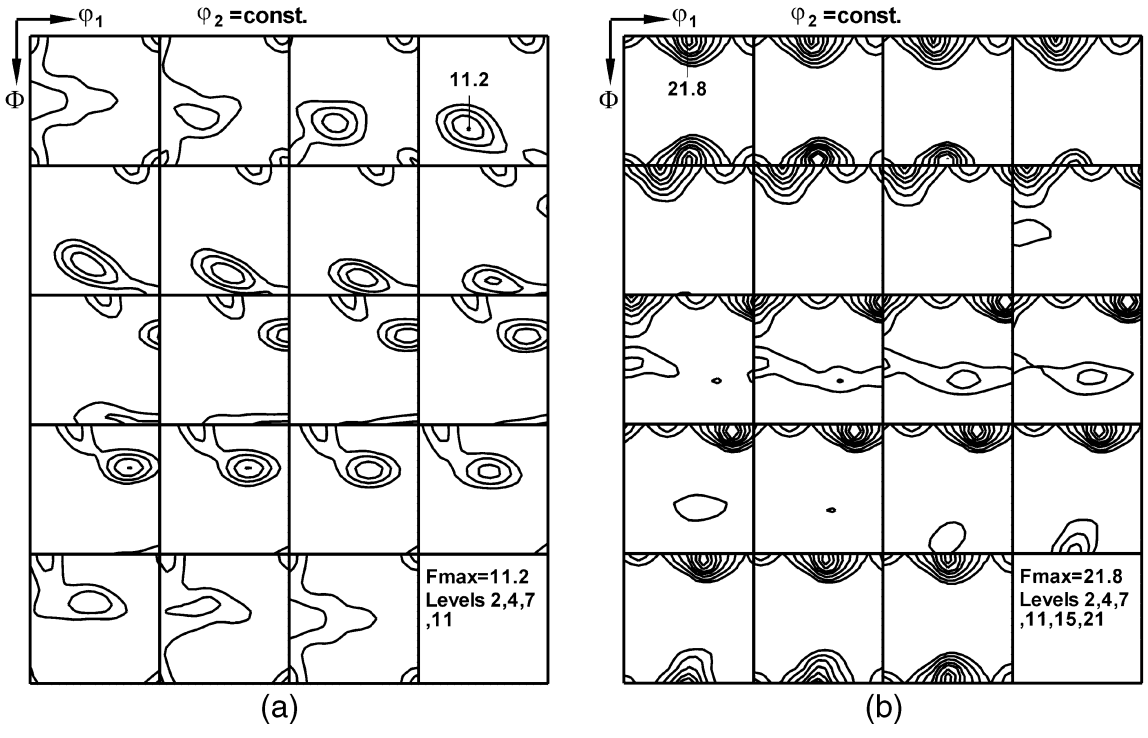

Figure 4 Simulated textures by using the strain states of (a) center layer and (b) 2/3 thickness layer.

rolling texture and shear textures. The maps of Taylor factors [9] discloses that the highest M is obtained at the $\{011\}\langle 011\rangle$ orientation for the strain states developing either the rolling texture or shear textures. Accordingly, the development of $\{011\}\langle 011\rangle$ at the surface layer ($s = 1.0$) of AA 3003 can be attributed to a preferred nucleation of recrystallization, which dominates the formation of recrystallization textures in the surface layers.

4. Summary

Three plies of sheets comprising two outer surfaces of STS 430 and inner middle of AA 3003 were produced by roll-cladding at 300°C and the evolution of through-thickness textures and microstructures in AA 3003 was studied. Roll-cladding led to pronounced texture gradients throughout the sample thickness of AA 3003: Strong cube-orientations and preferred orientations assembled along the β-fiber are observed in the center layer. Close to the sheet surfaces in contact with STS 430, the texture was characterized by the development of two distinct texture components of $\{011\}\langle 011\rangle$ and $\{001\}\langle 110\rangle$. Difference in strain states at different thickness layers and the subsequent recrystallization process during roll-cladding are responsible for the evolution of textures in AA 3003.

Acknowledgements

This work was supported by grant No. PS006-1-00-01 from the Center for Advanced Materials Processing (CAMP).

References

1. R. R. ARNOLD and P. W. WHITTON, *Proc. Inst. Mech. Eng.* **173** (1959) 241.
2. G. E. ARKULIS, "Compound Plastic Deformation of Layers of Different Metals" (Daniel Davey & Co., INC, New York, 1965).
3. V. RANDLE and O. ENGLER, "Introduction to Texture Analysis, Macrotexture, Microtexture and Orientation Mapping" (Gordon and Breach, Amsterdam, 2000).
4. H. J. BUNGE, "Texture Analysis in Materials Science" (Butterworths, London, 1982).
5. O. ENGLER, M. Y. HUH and C. N. TOMÉ, *Metall. Mater. Trans.* A **31** (2000) 2299.
6. J. HIRSCH and K. LÜCKE, *Acta Metall.* **36** (1988) 2883.
7. U. F. KOCKS, *Metall. Trans.* **1** (1970) 1121.
8. J. GIL SEVILLANO, P. VAN HOUTTE and E. AERNOUDT, *Prog. Mater. Sci.* **25** (1980) 69.
9. O. ENGLER, H. C. KIM and M. Y. HUH, *Mater. Sci. Technol.* **17** (2001) 74.
10. I. SAMAJDAR, B. VERLINDEN, P. VAN HOUTTE and D. VANDERSCHUEREN, *Mater. Sci. Eng.* A **238** (1997) 343.

Received 11 September 2003
and accepted 27 February 2004